# Kinetic studies on the formation of DNA triplexes containing the nucleoside analogue 2′-*O*-(2-aminoethyl)-5-(3-amino-1-propynyl)uridine

**David A. Rusling,[a] Victoria J. Broughton-Head,[a] Alex Tuck,[a] Hannah Khairallah,[a] Sadie D. Osborne,[b] Tom Brown[b] and Keith R. Fox*[a]**

*Received 30th August 2007, Accepted 18th October 2007*
*First published as an Advance Article on the web 1st November 2007*
**DOI: 10.1039/b713088k**

We have examined the kinetics of triple helix formation of oligonucleotides that contain the nucleotide analogue 2′-*O*-(2-aminoethyl)-5-(3-amino-1-propynyl)uridine (bis-amino-U, BAU), which forms very stable base triplets with AT. Triplex stability is determined by both the number and location of the modifications. BAU-containing oligonucleotides generate triplexes with extremely slow kinetics, as evidenced by 14 °C hysteresis between annealing and melting profiles even when heated at a rate as slow as 0.2 °C $min^{-1}$. The association kinetics were measured by analysis of the hysteresis profiles, temperature-jump relaxation and DNase I footprinting. We find that the slow kinetics are largely due to the decreased rate of dissociation; BAU modification has little effect on the association reaction. The sequence selectivity is also due to the slower dissociation of BAU from AT than other base pairs.

## Introduction

Triplex-forming oligonucleotides (TFOs) bind within the major groove of duplex DNA forming Hoogsteen hydrogen bonds with exposed groups on the base pairs.[1,2] Their unique base–base recognition properties make them ideal candidates as gene-recognition agents for exploitation in medicine and biotechnology.[2–7] The base composition of the oligonucleotide dictates its binding orientation and selectivity; those composed of pyrimidine bases bind in a parallel orientation to the purine-strand of the duplex, generating T.AT and $C^+$.GC triplets.[2] The application of these compounds is currently restricted by several intrinsic limitations. Under physiological pH and ionic conditions the binding of a TFO is weak, predominantly due to the requirement for cytosine protonation and charge repulsion between the three negatively charged strands. TFOs are also restricted to binding to oligopurine.oligopyrimidine sequences as there is no method for recognising TA or CG base pairs (pyrimidine inversions) using natural nucleotides. We and others have prepared nucleotide analogues to overcome these restrictions and have used these in combination to generate oligonucleotides which form stable triplexes at pH 7.0 at target sites which contain pyrimidine interruptions.[8–13]

As well as improving the overall stability of triplexes, the kinetic details of the binding of these modified TFOs is extremely important. The biological activities of these molecules will not only depend on increasing their affinity, but on their individual association and dissociation rates.[14] Ideally TFOs should bind rapidly to their target sites and dissociate very slowly, while their interaction with non-targeted sites must be much weaker and should be characterised by fast dissociation. In this manner they may be able to compete with, and selectively disrupt, the interaction of cellular DNA binding proteins, such as transcription factors and polymerases. It is known that the rate of triplex formation is very slow, about three orders slower than duplex formation.[15–19] It is also thought to proceed *via* a nucleation-zipper mechanism, dependent on the formation of a quasi-stable intermediate consisting of a few productive triplets, before a 'zippering' of the remainder of the third strand around the duplex helix.[20,21] The apparent rate of triplex association therefore decreases with temperature, as lower temperatures stabilise this intermediate. Triplex dissociation is also slow, with reports suggesting half lives of between 30 minutes and several days.[15–17,22–24]

In this study we have determined how the nucleoside analogue 2′-*O*-(2-aminoethyl)-5-(3-amino-1-propynyl)uridine (bis-amino-U; BAU: Fig. 1A) affects the kinetics of DNA triplex formation. Previous studies have shown that bis-amino-U binds to AT base pairs with a higher affinity and specificity than T.[25–27] Here we use fluorescence melting and DNase I footprinting experiments to assess the kinetic details of the interaction of TFOs containing this analogue with their intended target sites, and with sites that differ by a single base pair.

## Results

### BAU.AT triplets

**Hysteresis.** In previous studies[25] we showed that a single BAU substitution at the centre of TFO-2 increases the $T_m$ by about 7 °C and slows the kinetics so that there is still hysteresis between the melting and annealing profiles even with a rate of temperature change of only 0.067 °C $min^{-1}$. This hysteresis arises as a result of slow steps in the association and/or dissociation reactions. We have therefore analysed this hysteresis to estimate the individual association and dissociation rate constants. The fluorescence melting profiles for TFO-1 (central T.AT) and TFO-2 (central BAU.AT) are shown in Fig. 2. Both oligonucleotides produce hysteresis in their melting profiles, though note that in this Figure the complex with TFO-2 is heated 30 times slower

[a]*School of Biological Sciences, University of Southampton, Bassett Crescent East, Southampton, SO16 7PX, UK. E-mail: k.r.fox@soton.ac.uk; Fax: +44 23 8059 4459; Tel: +44 23 8059 4374*
[b]*School of Chemistry, University of Southampton, Highfield, Southampton, SO17 1BJ, UK*

 

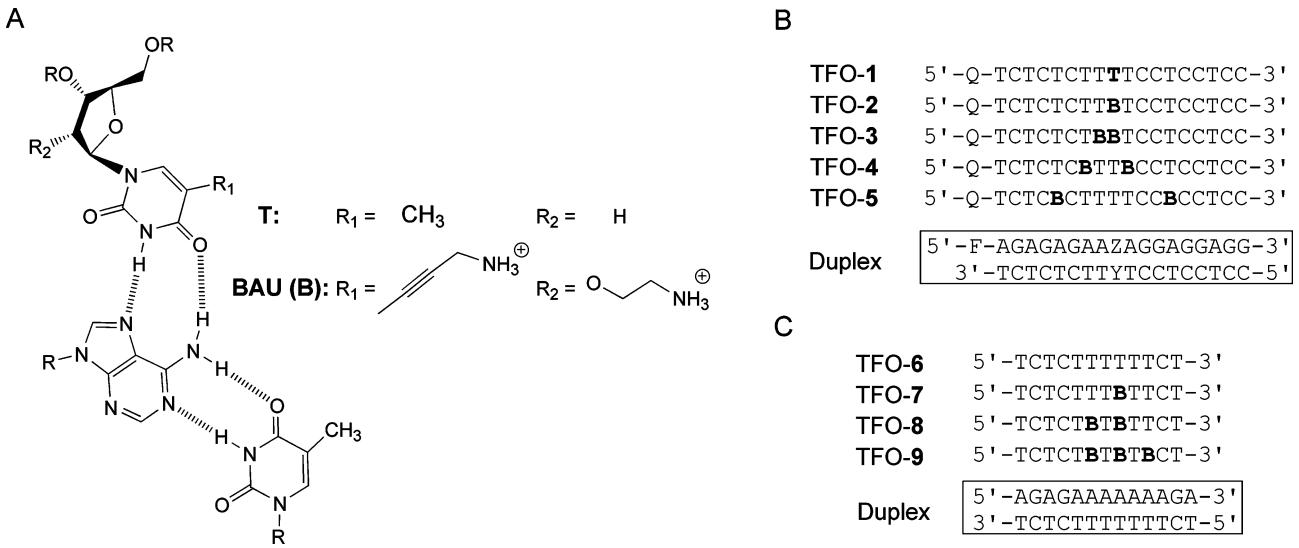


**Fig. 1** (A) Chemical structures of the T.AT and BAU.AT triplets. (B) Sequences of the oligonucleotides used in fluorescence melting and temperature jump experiments. The TFOs were labelled at the 5′-end with methyl red while the 5′-end of the purine-containing strand of each duplex was labelled with fluorescein. TFOs -2, -3, -4 and -5 contain one or two substitutions with BAU (B). The duplex is boxed and ZY corresponds to each of the four base pairs in turn. (C) Sequence of the oligonucleotides used in the footprinting experiments. TFOs -7, -8 and -9 contain one, two or three substitutions with BAU (B). The duplex target is boxed and is found within the 110 bp *tyrT*(43–59) DNA fragment. This fragment was labelled at the 3′-end with [α-$^{32}$P]dATP.

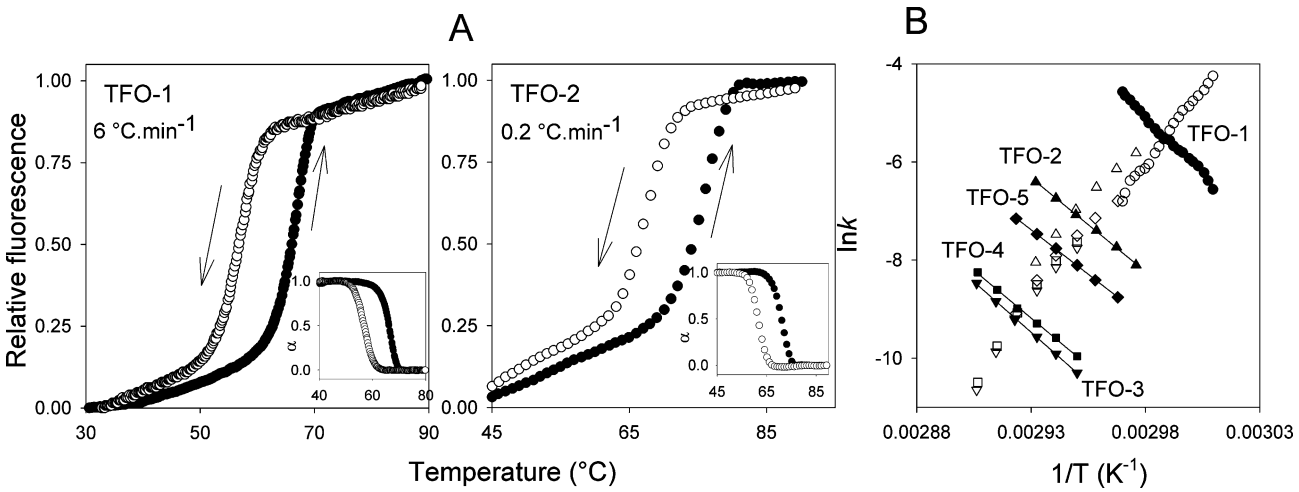


**Fig. 2** (A) Representative annealing (down arrow, open symbols) and heating (up arrow, filled symbols) profiles for the interaction of TFO-1 and TFO-2 with the duplex target shown in Fig. 1B, ZY = AT. The profiles for TFO-1 were obtained at a rate of temperature change of 6 °C min$^{-1}$ whilst the profiles for TFO-2 were determined at 0.2 °C min$^{-1}$. Fraction folded ($\alpha$) plots for each triplex are included in the insets. (B) Representative Arrhenius plots for the association ($k_1$) and dissociation ($k_{-1}$) constants for TFOs 1–5.

than that with TFO-1, demonstrating its much slower reaction kinetics. Arrhenius plots derived from these curves are shown in Fig. 2B. These plots are typical of those observed with other triplexes and display a negative slope for the dissociation reaction but a positive slope (apparent negative activation energy) for the association process. The apparent association rate ($k^*$) increases at lower temperatures and is explained by invoking a nucleation-zipper mechanism.[17] Since the measured association rate constant ($k^*$) is a complex of other primary rates, we will not comment on the absolute values, but note that the association rates are similar for both oligonucleotides, suggesting that BAU does not significantly affect the association process. In contrast the dissociation rate constants are in different regions on this Arrhenius plot confirming the much lower dissociation rate of BAU. The thermodynamic parameters for these dissociation processes are presented in Table 1, from which it can be seen that TFO-1 and TFO-2 have similar activation energies (evident in the similar slopes of the Arrhenius plots) and the major difference is in the pre-exponential factor A. The estimated dissociation half-lives of these TFOs at 37 °C differ by an order of magnitude.

The effect of including a second BAU substitution was examined using TFOs 3–5. The results are shown in Fig. 2 and Table 1. When the two BAU residues are close together or separated by two nucleotides (TFO-3 and TFO-4 respectively) the $T_m$ is increased further and the hysteresis becomes more pronounced. The Arrhenius plots for their association parameters lie on

**Table 1** Dissociation kinetic parameters estimated for the interaction of TFO 1–5 with the target duplex shown in Fig. 1B (ZY = AT). $T_m$ values were determined from fluorescence melting curves measured at 0.2 °C min$^{-1}$; in several instances there is hysteresis between the melting and annealing curves and the $T_m$s for annealing are shown in parentheses. The activation energy ($E_{off}$) and pre-exponential factor (A) were calculated from Arrhenius plots. These were derived from either the hysteresis between melting and annealing [determined at 6 °C min$^{-1}$ (TFO-1) or 0.2 °C min$^{-1}$ (TFO-2–5)] or from temperature-jump experiments. In the hysteresis experiments the TFO concentration was 3 μM and the duplex was 0.25 μM. For the temperature-jump data the TFO concentration was 0.25 μM and the duplex was 0.25 μM. All reactions were performed in 50 mM sodium acetate pH 5.0 containing 200 mM NaCl

| | | Hysteresis | | | | Temperature-jump | |
|---|---|---|---|---|---|---|---|
| TFO | $T_m$/°C | $E_{off}$/kJ mol$^{-1}$ | LnA | $^{37}k_{-1}$/s$^{-1}$ | $^{37}t_{1/2}$/s | $E_{off}$/kJ mol$^{-1}$ | LnA |
| 1 | 63.8 (63.4) | 362 ± 4 | 125 ± 3 | $1.9 \times 10^{-7}$ | $3.6 \times 10^{6}$ | 427 ± 12 | 148 ± 5 |
| 2 | 70.4 (64.6) | 340 ± 12 | 114 ± 4 | $1.7 \times 10^{-8}$ | $4.2 \times 10^{7}$ | 418 ± 6 | 140 ± 2 |
| 3 | 78.4 (64.1) | 332 ± 12 | 108 ± 4 | $9.1 \times 10^{-10}$ | $7.6 \times 10^{8}$ | | |
| 4 | 77.8 (64.8) | 300 ± 11 | 97 ± 4 | $3.8 \times 10^{-9}$ | $1.8 \times 10^{8}$ | | |
| 5 | 73.0 (64.9) | 291 ± 14 | 95 ± 4 | $1.7 \times 10^{-8}$ | $4.1 \times 10^{7}$ | | |

the same line as for TFO-1 and TFO-2, confirming that these modifications have little or no effect on the association reaction. In contrast the dissociation rates are even slower. Surprisingly the activation energies are slightly lower than for TFO-1 and TFO-2 (which alone would lead to a faster dissociation rate) and the main effect is in the pre-exponential factor (A). Separating the two BAU residues by seven nucleotides (TFO-5) does not increase the $T_m$ relative to TFO-2; the activation energy is lowered as too is the pre-exponential factor. In this case these two effects cancel each other and TFO-2 and TFO-5 display similar dissociation half lives. The faster dissociation of TFO-5 compared to TFO-3 and TFO-4 could either be due to the greater separation of the two BAU residues or the nature of the flanking triplets. In TFO-4 each BAU.AT triplet is flanked by T.AT and C$^+$.GC, while in TFO-5 both BAU.AT triplets are flanked by C$^+$.GC on each side.

**Temperature-jump.** We further explored the kinetics of triplex formation by these TFOs by performing temperature jump experiments on the same complexes.[15] In these experiments the complexes are first equilibrated at a temperature about 10 °C below the $T_m$ (estimated as the midpoint between the value for the annealing and melting reactions); the temperature is then rapidly increased by 5 °C and the changes in fluorescence are recorded as the system relaxes to a new equilibrium. Representative relaxation curves for TFO-1 and TFO-2 are shown in Fig. 3 for different concentrations of each TFO. Each of these reaction profiles was adequately fitted by a single exponential curve and Arrhenius plots derived from these data are shown in Fig. 4A. For a simple process the relaxation rate constant is equal to the sum of the association and dissociation rates ($k_1$[TFO] + $k_{-1}$). Since $k_1$ has a negative activation energy (as shown above), the Arrhenius plots have a parabolic shape with a minimum at the $T_m$ (where $k_1$[TFO] = $k_{-1}$); at temperatures below the $T_m$ $k_1$[TFO] is greater than $k_{-1}$ and the rate is dominated by the association rate constant, whereas at higher temperatures $k_{-1} > k_1$[TFO] and the relaxation rate is dominated by $k_{-1}$. The upturn in the Arrhenius plots at low temperatures (to the right of the graph) is more pronounced at higher TFO concentrations as the apparent association rate increases. At temperatures below the $T_m$ the Arrhenius plots are linear at low oligonucleotide concentrations (for which association will be slowest) and these were used to determine the kinetic parameters for TFO-1 (T.AT) and TFO-2 (BAU.AT) that are presented in Table 1. Although the values of $E_a$ and A are about 30% higher than those determined from the hysteresis

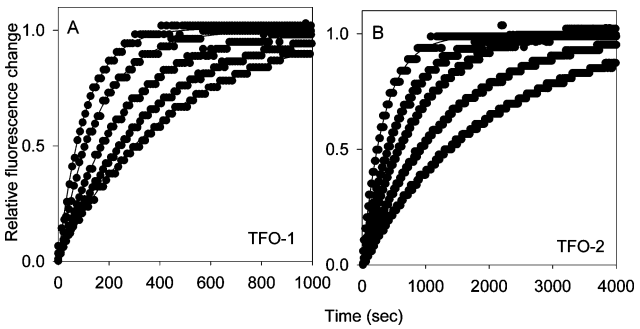


**Fig. 3** Representative temperature-jump profiles for the interaction of TFO-1 (panel A) and TFO-2 (panel B) with the target site containing a central AT base pair. The TFO and target duplex concentrations were both 0.25 μM. Each curve was obtained by rapidly increasing the temperature by 5 °C, measuring the time-dependent increases in fluorescence. The final temperatures were 60, 61, 62, 63 and 64 °C for TFO-1 and 66, 67, 68, 69 and 70 °C for TFO-2, each increasing from right to left.

experiments, they follow the same pattern. The dominant factor that is responsible for the slow dissociation of BAU is the pre-exponential factor not the activation energy.

Similar experiments with TFO-3, TFO-4 and TFO-5 confirm the results from the hysteresis experiments. Representative temperature-jump relaxation curves for all five oligonucleotides at 70 °C are presented in Fig. 4B. These show similar profiles for TFO-3 and TFO-4, which are both slower than TFO-2, while TFO-5, in which the two BAU residues are separated by a greater distance and flanked by C$^+$.GC triplets has similar properties to TFO-2. Arrhenius plots derived from the relaxation profiles with 3 μM TFO-3–5 are shown in Fig. 4A. It can be seen that the linear portions of these plots (at high temperatures) have similar slopes (activation energies), but are in different positions on the graph. TFO-3 (inverted diamonds) and TFO-4 (squares) are very similar, while TFO-5 (diamonds) shows faster dissociation.

## BAU triplet mismatches

We have previously demonstrated that BAU retains the selectivity for AT base pairs and has enhanced discrimination against CG and TA base pairs.[25] We therefore examined whether this discrimination results from changes in the association or dissociation rates and performed hysteresis and temperature-jump experiments with TFO-1 and TFO-2 using duplex targets, in which the central

 

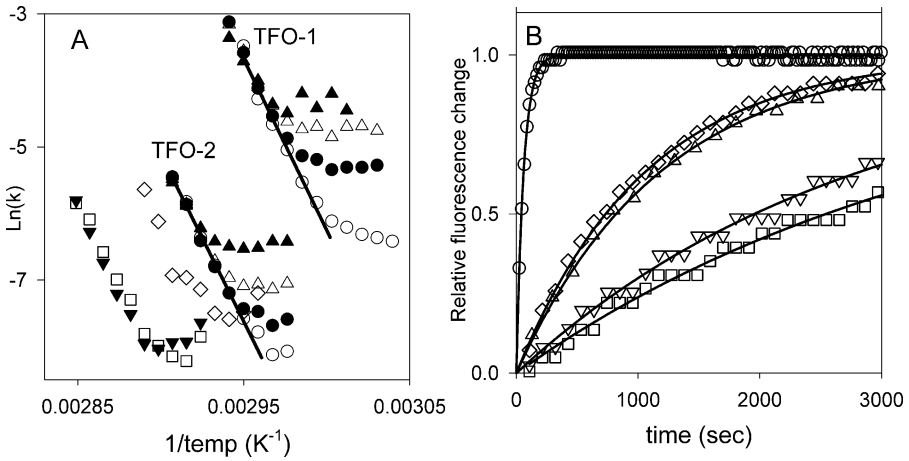


**Fig. 4** (A) Arrhenius plots showing the temperature dependence of the relaxation rate constants for TFO-1–5. The concentrations of TFO-1 and TFO-2 were 0.25 μM (open circles), 1 μM (filled circles), 3 μM (open triangles) 10 μM (filled triangles). For TFO-3 (inverted triangles), TFO-4 (squares) and TFO-5 (diamonds) data for 3 μM oligonucleotide are presented. (B) Representative temperature-jump profiles for the interaction of TFOs 1–5 with the target site containing a central AT base pair. The TFO concentration was 0.25 μM in each case and the temperature was rapidly increased from 65 to 70 °C. TFO-1 (circles), TFO-2 (triangles), TFO-3 (inverted triangles), TFO-4 (squares), TFO-5 (diamonds).

base pair was exchanged for each base pair in turn. Arrhenius plots for the complexes containing these triplex mismatches are presented in Fig. 5. A full quantitative analysis of these data is not possible since, as we have previously noted, the melting curves for complexes that contain triplex mismatches are biphasic,[25] as the triplex melts at much lower temperatures than the duplex. The estimated kinetic parameters therefore contain large systematic errors and so can only be used for a qualitative comparison of the different complexes. Once again the association kinetics (derived from the hysteresis profiles) show negative activation energies and, although the individual curves do not overlap, they are in similar regions (unlike the dissociation profiles). For TFO-1 the association plots have similar slopes and those for T.CG and T.TA are almost contiguous. Since the Arrhenius plots for the association reaction are clearly not measuring primary kinetic events they were not analysed further. In contrast the Arrhenius plots for the dissociation reactions show clear differences between the targets, with similar results obtained by the two techniques. Looking first at the results for TFO-1 it can be seen that T.TA has a faster dissociation than T.GC or T.CG, which are faster than T.AT. The slower dissociation of T.CG may not be surprising since this triplet has been used as a (poor) means of recognising CG inversions. The slow dissociation of T.GC is also consistent with the reported $T_m$ values of TFOs that contain this triplet, which are similar to those containing T.CG.[25,28] For TFO-2, which contains a central BAU residue, the association plots are again almost contiguous, though with different slopes. As for TFO-1 the dissociation plots for the four targets have different rates. BAU.AT is much slower than the other three, though GC is considerably slower than both BAU.TA and BAU.CG, which have similar profiles. It is clear that, at these elevated temperatures around the $T_m$ of each complex, the major differences between the matched and mismatched complexes arise from changes in the dissociation, rather than the association rates.

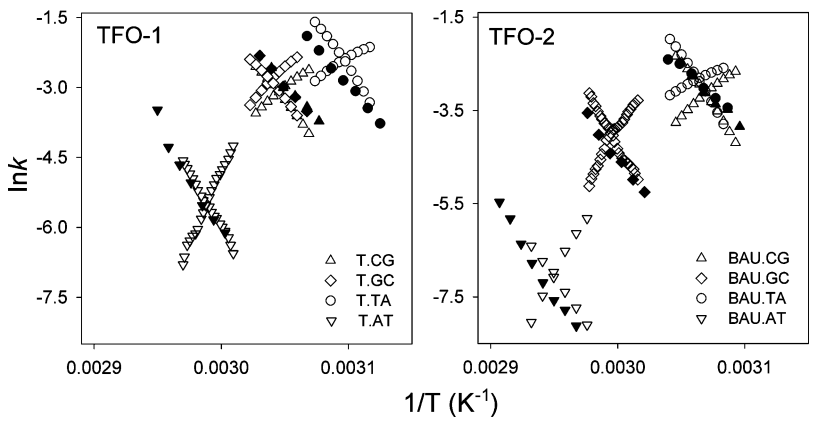


**Fig. 5** Arrhenius plots for the interaction of TFO-1 and TFO-2 with target sites containing ZY as each base pair in turn. Open symbols correspond to data obtained from hysteresis experiments (TFO concentration 3 μM), whilst closed symbols correspond to data obtained from temperature-jump experiments (TFO concentration 0.25 μM). ZY = CG (triangles); GC (diamonds) and TA (circles). The data from T.AT and B.AT are taken from Fig. 3 and 4. The dissociation data lie on lines with negative slopes, while the association data show positive slopes. The association data correspond to the measured pseudo first-order rate constant $k^* = k_1$[TFO].

### DNase I footprinting

**Association.** We further compared the slow association rates of BAU-containing TFOs by performing DNase I footprinting reactions at different times after mixing the TFOs with a radiolabelled fragment containing the target site.[16,24] Typical association reaction profiles for TFO-6 and TFO-7, containing a central T or BAU respectively, are presented in Fig. 6, showing the slow appearance of the footprint. The plots of relative band intensity against time were fitted with exponential curves (Fig. 6B), providing the apparent rate constants ($k_{obs}$). These observed rate constants are dependent on the total nucleic acid concentration ($k_{obs} = k_{-1} + k_1[NA]$) and the insets to Fig. 6B show the concentration dependence of the apparent rate constants, from which the values of $k_1$, presented in Table 2 were estimated. The values of these association rate constants, around $10^3$ $M^{-1}$ $s^{-1}$, are similar to those reported in other studies. The association rates, which are dependent on the magnesium concentration, are similar for TFO-6 and TFO-7, confirming that the addition of a single BAU residue does not significantly alter the association reaction. In contrast to the hysteresis and temperature-jump data TFO-8, containing two BAU residues and TFO-9, with three BAUs appear to form faster than TFO-6 or TFO-7.

**Dissociation.** We observed the slow kinetics of dissociation of TFO-6 and TFO-7 by adding a 10-fold excess of an oligonucleotide complementary to the third strand, thereby sequestering the free TFO as a short duplex and preventing its re-association with the target duplex. The results of these experiments are shown in Fig. 7 and Table 2. At 20 °C the unmodified TFO-6 dissociated with a half-life of about 50 minutes. In contrast no dissociation of TFO-7, containing one BAU residue, was detected even after overnight incubation. On increasing the temperature to 30 °C dissociation of TFO-6 was too fast to measure, while TFO-7 dissociated with a half-life of about 30 minutes. No dissociation was detected for TFO-8 or TFO-9 even at 30 °C.

**Table 2** Association and dissociation rate constants for the interaction of TFOs 6–9 with the target site in the *tyr*T(43–59) fragment determined by DNase I footprinting. The reactions were performed in 50 mM sodium acetate, pH 5.0 containing 200 mM NaCl and 2.5 mM (*) or 5 mM (#) $MgCl_2$ at 20 °C, except for † which was measured at 30 °C

| TFO | $k_1/M^{-1}$ $s^{-1}$ | $k_{-1}/s^{-1}$ |
|---|---|---|
| *6 | $2.4 \times 10^3$ | $2.4 \times 10^{-4}$ |
| *7 | $3.8 \times 10^3$ | †$3.6 \times 10^{-4}$ |
| #6 | $0.7 \times 10^3$ | |
| #7 | $0.6 \times 10^3$ | |
| #8 | $2.0 \times 10^3$ | |
| #9 | $1.0 \times 10^4$ | |

## Discussion

These results demonstrate that the enhanced stability of triplexes containing the BAU.AT triplet relative to T.AT is largely due to its slower dissociation rather than changes in the association reaction. Surprisingly we find that the activation energy for the dissociation reaction is largely unaffected by introducing a single BAU modification and the slower dissociation is mainly due to a decrease in the pre-exponential factor (A). The similar values of $E_a$ for TFOs 1 and 2 may not be surprising as they only differ by a single modification at the centre of the oligonucleotides and this region may not be involved in the primary dissociation event. Since the pre-exponential factor is a function of the entropy of

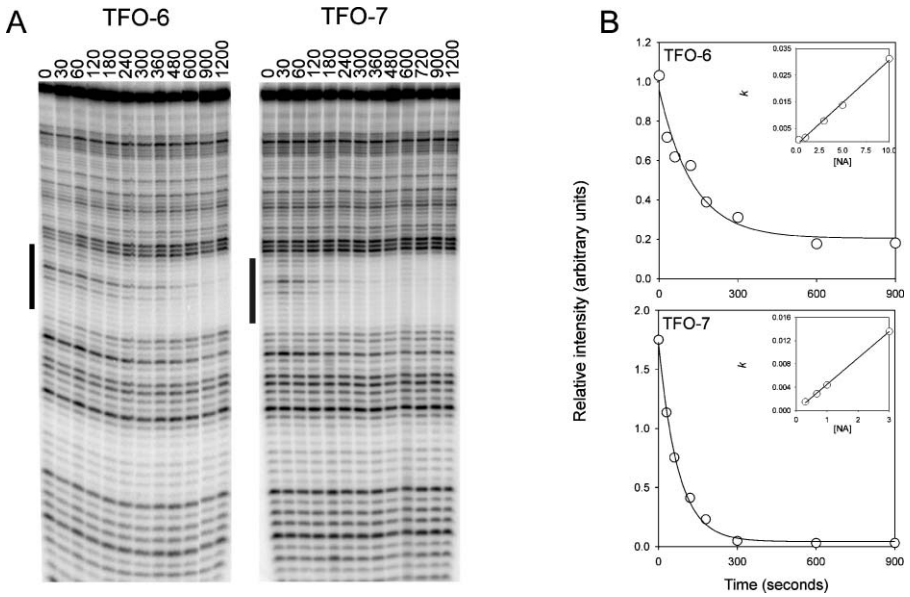


**Fig. 6** Determination of TFO association rates by DNase I footprinting. (A) DNase I cleavage patterns of the *tyr*T(43–59) DNA fragment in the presence of 3 μM of TFO-6 and 7 at different times after adding the TFOs. The experiments were performed at 20 °C. The time (sec) after adding the TFO is indicated at the top of each gel lane. The black bars show the TFO target site. (B) Plots of relative band intensity within the footprint against time for each TFO. The insets show the concentration dependence of the apparent rate constants, from which the association rate constants, listed in Table 4, were derived.

 

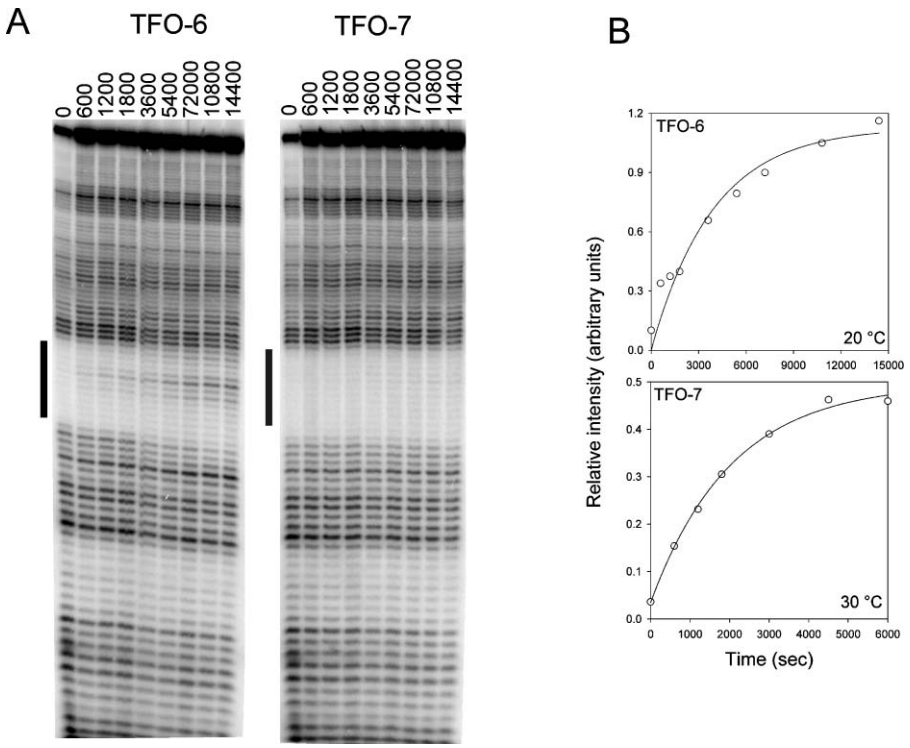


**Fig. 7** Determination of TFO dissociation rates by DNase I footprinting. (A) DNase I cleavage patterns of the *tyr*T(43–59) DNA fragment in the presence of 3 μM of TFO-6 and 7. The complexes were equilibrated overnight at 20 °C before adding 30 μM of the complementary oligonucleotide 3′-AGAGAAAAAAGA. The time (sec) after adding the complementary oligonucleotides is shown at the top of the gel lanes. The black bars indicate the TFO target site. (B) Plots of relative band intensity within the footprint against time for each TFO. The data for TFO-6 were obtained at 20 °C, while those for TFO-7 correspond to 30 °C.

the activated state, this suggests that the enhanced stability of BAU.AT may arise from the conformational organisation of the third strand.

These conclusions relate to a given set of experimental conditions (200 mM NaCl and pH 5.0). The difference between the BAU and T bases may be altered at different salt concentrations or pH. Since BAU provides two more positive charges than T the differences may be magnified at lower ionic strengths, but reduced at higher pH.

TFO-3 and TFO-4, in which the two BAU residues are adjacent or separated by two nucleotides, show similar properties, though the dissociation half-life for TFO-3 is longer. This is consistent with studies with psoralen-linked TFOs that contain 2′-aminoethoxy-T, which produce more stable complexes when the modifications are close together,[14,29] but contrasts to our previous work which suggested that the most stable complexes are produced when these modifications are evenly distributed along the third strand.[26] Further increasing the distance between the two BAU residues (TFO-5) generates less stable complexes (equivalent to the TFO containing only one BAU residue), though this may also be due to the presence of $C^+$.GC triplets adjacent to BAU.AT in TFO-5. Although the stability of T.AT triplets is enhanced by the presence of adjacent $C^+$.GC triplets,[15,30] analogues that bear positively charged groups can be inhibited by adjacent $C^+$.GC triplets.[31]

The results with targets that generate triplet mismatches provide further information on the stringency of BAU. This base analogue is highly selective for AT relative to other base pairs, though it binds better to GC than CG or TA.[25] In contrast T.GC and T.CG are more stable than T.TA. It is not clear why BAU stabilises the interaction with GC but not CG, especially since the T.CG triplet is known to provide the best means for recognizing CG inversions using natural bases.[32,33] It is possible that the additional contacts or structural changes provided by BAU are not compatible with the single hydrogen bond that is formed in the T.CG triplet. Once again it is clear that discrimination between the different base pairs is a consequence of changes in the dissociation, rather than association, rate constants.

It is not possible to compare the results from footprinting with those from hysteresis and temperature-jump experiments as they used different length oligonucleotides (12-mers and 18-mers). The ratio of $k_{-1}$–$k_1$ derived from the footprinting experiments gives a value of 0.1 μM, which is similar to the dissociation constant of this oligonucleotide.

Effective DNA triple helix formation *in vivo* will require not only strong equilibrium binding, which we have achieved by using the positively charged nucleotide analogue BAU, but fast association (competing with various DNA binding proteins) and long dissociation half-lives. The results presented in this paper demonstrate that stability of the BAU.AT triplet is achieved by slowing the dissociation reaction, with little effect on the association kinetics. Different nucleic acid derivatives, or the inclusion of many more modifications, will be required to improve on the slow association kinetics.

## Experimental

### Oligonucleotides

All oligonucleotides were synthesized on an Applied Biosystems ABI 394 automated DNA/RNA synthesizer on the 0.2 μmol or 1 μmol scale using the standard cycles of acid-catalysed detritylation, coupling, capping and iodine oxidation procedures. Phosphoramidite monomers and reagents were purchased from Applied Biosystems or Link Technologies. The phosphoramidite for BAU was prepared as previously reported.[25,27] The oligonucleotides were deprotected for 24 h in 2 ml of 30% aqueous methylamine in the presence of phenol (5 mg). The deprotected oligonucleotides were purified by reverse-phase HPLC on a Brownlee Aquapore column (C8) using a gradient of acetonitrile in 0.1 M ammonium acetate. Purified oligonucleotides were analysed by MALDI-TOF mass spectrometer in positive ion mode using internal $T_n$ standards.[34] The sequences of the oligonucleotides used in this work are shown in Fig. 1.

### Fluorescence melting experiments

Kinetic parameters for the intermolecular triplexes shown in Fig. 1B were obtained using fluorescence melting and temperature-jump experiments as previously described.[13,15,28,35] TFOs were labelled at the 5′-end with methyl red and the 5′-end of the purine-containing strand of each duplex was labelled with fluorescein. The triplexes were prepared in 50 mM sodium acetate buffer containing 200 mM sodium chloride at pH 5.0. Melting experiments were carried out in a total volume of 20 μl and each assay contained 0.25 μM duplex and 3 μM third strand (unless otherwise stated).

**Hysteresis experiments.** The method for estimating kinetic parameters from non-equilibrium melting and annealing curves has previously been reported.[17,36,37] The hysteresis between these curves arises because the complexes are heated or cooled at a rate that is too fast to allow thermodynamic equilibrium, and indicates the presence of slow steps in the association and/or dissociation reactions. For triplexes, the extent of this hysteresis is dependent on a range of factors such as the pH, the concentration of divalent metal ions and the sequence context.

To ensure correct annealing, the triplexes were initially heated to 95 °C and then slowly cooled to room temperature. Although the slowest rate of continuous temperature change by the LightCycler is 0.1 °C sec$^{-1}$, slower rates were obtained by increasing/decreasing the temperature in 1 °C steps, leaving the samples to equilibrate for a suitable length of time (typically 5 min). Hysteresis curves were then obtained by heating the samples at a fast rate (typically 6 °C min$^{-1}$) to 95 °C, leaving the samples to equilibrate for 5 min, and then cooling the samples to 35 °C at the same rate. Recordings were taken during both the heating and cooling cycles. The rate of temperature change was adjusted for each triplex so as to obtain optimal separation between the melting and annealing curves. $T_m$ values were determined from the first derivatives of the melting profiles using the software provided. If $a_c$ and $a_h$ are the fractions of the duplex that are occupied by the third strand in the cooling and heating curves respectively, then $d(a_c)/dT = d(a_c)/dt \times (dT/dt)^{-1}$ and $d(a_h)/dT = d(a_h)/dt \times (dT/dt)^{-1}$, where $t$ is time and $T$ is temperature. If $k_1$ and $k_{-1}$ are the triplex association and dissociation rate then $d(a_c)/dt = k_1[TFO](1 - a_c) - k_{-1}a_c$ and $d(a_h)/dt = k_1[TFO](1 - a_h) - k_{-1}a_h$. By measuring $d(a_c)/dT$, $d(a_h)/dT$, $a_c$ and $a_h$, the individual rate constants can be estimated at each temperature.[17,36,37] Since the third strand concentration is in excess in these experiments it effectively remains constant during the reaction (3 μM), yielding a pseudo first order process with a rate constant $k^*$ given by $k_1[TFO]$. In several instances the melting curves revealed a biphasic profile corresponding to dissociation of the duplex (with a decrease in fluorescence intensity) at higher temperatures than dissociation of the third strand as previously noted.[25,35] This was especially noticeable with complexes that contained a triplex mismatch. These were fitted by assuming a coupled equilibrium in which the third strand dissociates first yielding a species with high fluorescence, followed by dissociation of the underlying duplex producing a random coil with a lower fluorescence.

**Temperature-jump experiments.** The dissociation kinetics of these intermolecular triplexes were determined by rapidly increasing the temperature and following the subsequent slow changes in fluorescence as the system relaxes to a new equilibrium.[15,38,39] In these experiments, the temperature was first increased slowly to a temperature ~10 °C below the $T_m$, and then left to equilibrate for 10 minutes. The temperature was then rapidly increased by 5 °C (at 20 °C sec$^{-1}$) recording the fluorescence as the system relaxes to a new equilibrium. This temperature change causes some of the triplex to dissociate, producing an increase in fluorescence intensity. Successive temperature jumps were then recorded on the same sample. The time-dependent changes in fluorescence were fitted by an exponential function $F_t = F_0 + F_f \times (1 - e^{-kt})$ where $F_0$ is the initial fluorescence, $F_t$ is fluorescence at time and $F_f$ is final fluorescence. The temperature jump experiments each contained 0.25 μM intramolecular duplexes and between 0.25 and 10 μM triplex-forming oligonucleotide. The observed relaxation rate constant ($k$) will be a function of the oligonucleotide concentration, the dissociation ($k_{-1}$) and association ($k_1$) rate constants, according to the equation $k = k_{-1} + k_1[DNA]$, where [DNA] is the total oligonucleotide concentration (third strand plus duplex). Values of $k_1$ and $k_{-1}$ at each temperature were determined from the slope of plots of $k$ against [DNA]. Arrhenius plots for the dissociation constants ($k_{-1}$) showed the expected linear relationship between $\ln(k_{-1})$ and $1/T$, from which activation energies were derived and values at 37 °C were obtained by extrapolation.

### Quantitative DNase I footprinting experiments

**DNA fragments.** The *tyr*T(43–59) fragment contains a 17-base oligopurine tract between positions 43 and 59.[40] We have targeted a 12 base pair region within this tract with the TFOs shown in Fig. 1C. A 110 base pair radiolabelled fragment containing this sequence was obtained by digesting the plasmid with *Eco*RI and *Ava*I and labelling at the 3′-end of the *Eco*RI site using reverse transcriptase and [α-$^{32}$P]dATP. This was then separated from the remainder of the plasmid DNA on an 8% (w/v) non-denaturing polyacrylamide gel. After elution the fragment was dissolved in 10 mM Tris-HCl, pH 7.5, containing 0.1 mM EDTA to give about 10 cps μl$^{-1}$ as determined on a hand held Geiger counter (<nM).

**Association reactions.** The association reactions were initiated by mixing 30 μl of oligonucleotide (between 0.1 and 10 μM) with 15 μl of radiolabelled DNA at 20 °C.[16,24] The oligonucleotides

 

were diluted in 50 mM sodium acetate pH 5.0 containing 5 mM magnesium chloride unless otherwise stated. The association reaction was followed by removing 3 µl aliquots at various time points (between 30 sec and 4 h) and digesting with 2 µl of DNase I for 20 seconds (typically ~0.05 units per mL, diluted in 200 mM NaCl containing 2 mM $MgCl_2$ and 2 mM $MnCl_2$). The reaction was stopped by adding 4 µl of 80% formamide containing 10 mM EDTA, 10 mM NaOH and 0.1% (w/v) bromophenol blue.

**Dissociation reactions.** Triplexes were formed by mixing 30 µl of appropriately diluted oligonucleotide (typically 3 µM) with 15 µl of radiolabelled DNA, and equilibrating overnight at an appropriate temperature (20 or 30 °C). Dissociation was initiated by adding a 10-fold excess of an oligonucleotide complementary to the third strand, thereby sequestering the free TFO as a short duplex.[24,41] Since duplex formation is much faster than triplex formation, the rate of disappearance of the footprint corresponds to the dissociation of the third strand from its target. The reaction was followed by removing 3 µl aliquots at various time points (between 30 sec and 4 h) and digesting with DNase I as above.

**Gel electrophoresis.** The products of digestion were separated on 10% polyacrylamide gels containing 8 M urea. Samples were heated to 100 °C for 3 min, before rapidly cooling on ice and loading onto the gel. Polyacrylamide gels (40 cm long, 0.3 mm thick) were run at 1500 V for about 2 h and then fixed in 10% (v/v) acetic acid. These were transferred to Whatman 3 MM paper and dried under vacuum at 86 °C for 1 h. The dried gels were subjected to phosphorimaging using a Molecular Dynamics Storm phosphorimager.

**Quantitative analysis.** The association of the oligonucleotide with its target site is revealed by the time-dependent appearance of a footprint, while the dissociation is revealed by the time-dependent disappearance of a footprint. The intensity of bands within each footprint was estimated using ImageQuant software. These intensities were then normalised relative to a band in the digest which is not part of the triplex target site, and which was not affected by addition of the oligonucleotides. For the association reaction, pseudo-first order rate constants ($k_{app}$) were estimated by fitting single exponential curves to the plots of band intensity against time using SigmaPlot. Bimolecular rate constants ($k_1$) were estimated from the variation of the observed rate constants with oligonucleotide concentration. For the dissociation reaction, the first order rate constants ($k_{-1}$) were estimated by fitting single exponential curves to the plots of band intensity against time using Sigmaplot.

## Acknowledgements

This work was funded by the BBSRC and EU grant LSHB-CT-2004-005204. Alex Tuck was supported by a Wellcome Vacation Studentship.

## References

1 G. Felsenfeld, D. R. Davies and A. Rich, *J. Am. Chem. Soc.*, 1957, **79**, 2023–2024.
2 H. E. Moser and P. B. Dervan, *Science*, 1987, **238**, 645–650.
3 S. Buchini and C. J. Leumann, *Curr. Opin. Chem. Biol.*, 2003, **7**, 717–726.
4 J. Y. Chin, E. B. Schleifman and P. M. Glazer, *Front. Biosci.*, 2007, **12**, 4288–4297.
5 K. R. Fox, *Curr. Med. Chem.*, 2000, **7**, 17–37.
6 C. Helene and J. J. Toulme, *Biochim. Biophys. Acta*, 1990, **1049**, 99–125.
7 M. M. Seidman and P. M. Glazer, *J. Clin. Invest.*, 2003, **112**, 487–494.
8 S. Buchini and C. J. Leumann, *Angew. Chem., Int. Ed.*, 2004, **43**, 3925–3928.
9 K. R. Fox and T. Brown, *Q. Rev. Biophys.*, 2005, **38**, 311–320.
10 D. M. Gowers and K. R. Fox, *Nucleic Acids Res.*, 1999, **27**, 1569–1577.
11 J. S. Li, F. X. Chen, R. Shikiya, L. A. Marky and B. Gold, *J. Am. Chem. Soc.*, 2005, **127**, 12657–12665.
12 J. Robles, A. Grandas, E. Pedroso, F. J. Luque, R. Eritja and M. Orozco, *Curr. Org. Chem.*, 2002, **6**, 1333–1368.
13 D. A. Rusling, V. E. C. Powers, R. T. Ranasinghe, Y. Wang, S. D. Osborne, T. Brown and K. R. Fox, *Nucleic Acids Res.*, 2005, **33**, 3025–3032.
14 M. M. Seidman, N. Puri, A. Majumdar, B. Cuenoud, P. S. Miller and R. Alam, *Ann. N. Y. Acad. Sci.*, 2005, **1058**, 119–127.
15 P. L. James, T. Brown and K. R. Fox, *Nucleic Acids Res.*, 2003, **31**, 5598–5606.
16 H. M. Paes and K. R. Fox, *Nucleic Acids Res.*, 1997, **25**, 3269–3274.
17 M. Rougee, B. Faucon, J. L. Mergny, F. Barcelo, C. Giovannangeli, T. Garestier and C. Helene, *Biochemistry*, 1992, **31**, 9269–9278.
18 H. Shindo, H. Torigoe and A. Sarai, *Biochemistry*, 1993, **32**, 8963–8969.
19 L. E. Xodo, *Eur. J. Biochem.*, 1995, **228**, 918–926.
20 P. Alberti, P. B. Arimondo, J. L. Mergny, T. Garestier, C. Helene and J. S. Sun, *Nucleic Acids Res.*, 2002, **30**, 5407–5415.
21 D. Porschke and M. Eigen, *J. Mol. Biol.*, 1971, **62**, 361–381.
22 C. Ellouze, F. Piot and M. Takahashi, *J. Biochem.*, 1997, **121**, 521–526.
23 L. J. Maher, P. B. Dervan and B. J. Wold, *Biochemistry*, 1990, **29**, 8820–8826.
24 E. Protozanova and R. B. Macgregor, *Anal. Biochem.*, 1996, **243**, 92–99.
25 S. D. Osborne, V. E. C. Powers, D. A. Rusling, O. Lack, K. R. Fox and T. Brown, *Nucleic Acids Res.*, 2004, **32**, 4439–4447.
26 D. A. Rusling, L. Le Strat, V. E. C. Powers, V. J. Broughton-Head, J. Booth, O. Lack, T. Brown and K. R. Fox, *FEBS Lett.*, 2005, **579**, 6616–6620.
27 M. Sollogoub, R. A. J. Darby, B. Cuenoud, T. Brown and K. R. Fox, *Biochemistry*, 2002, **41**, 7224–7231.
28 D. A. Rusling, T. Brown and K. R. Fox, *Biophys. Chem.*, 2006, **123**, 134–140.
29 N. Puri, A. Majumdar, B. Cuenoud, P. S. Miller and M. M. Seidman, *Biochemistry*, 2004, **43**, 1343–1351.
30 R. W. Roberts and D. M. Crothers, *Proc. Natl. Acad. Sci. U. S. A.*, 1996, **93**, 4320–4325.
31 D. M. Gowers, J. Bijapur, T. Brown and K. R. Fox, *Biochemistry*, 1999, **38**, 13747–13758.
32 I. Radhakrishnan and D. J. Patel, *J. Mol. Biol.*, 1994, **241**, 600–619.
33 K. Yoon, C. A. Hobbs, J. Koch, M. Sardaro, R. Kutny and A. L. Weis, *Proc. Natl. Acad. Sci. U. S. A.*, 1992, **89**, 3840–3844.
34 G. J. Langley, J. M. Herniman, N. L. Davies and T. Brown, *Rapid Commun. Mass Spectrom.*, 1999, **13**, 1717–1723.
35 R. A. J. Darby, M. Sollogoub, C. McKeen, L. Brown, A. Risitano, N. Brown, C. Barton, T. Brown and K. R. Fox, *Nucleic Acids Res.*, 2002, **30**, e39.
36 E. Bernal-Mendez and C. J. Leumann, *Biochemistry*, 2002, **41**, 12343–12349.
37 A. De Cian, L. Guittat, M. Kaiser, B. Sacca, S. Amrane, A. Bourdoncle, P. Alberti, M. P. Teulade-Fichou, L. Lacroix and J. L. Mergny, *Methods*, 2007, **42**, 183–195.
38 N. M. Brown, P. A. Rachwal, T. Brown and K. R. Fox, *Org. Biomol. Chem.*, 2005, **3**, 4153–4157.
39 E. E. Merkina and K. R. Fox, *Biophys. J.*, 2005, **89**, 365–373.
40 P. M. Brown, C. A. Madden and K. R. Fox, *Biochemistry*, 1998, **37**, 16139–16151.
41 M. C. Fletcher and K. R. Fox, *FEBS Lett.*, 1996, **380**, 118–122.